Pergamon

www.elsevier.com/locate/jaerosci

PII: S0021-8502(99)00026-9

J. Aerosol Sci. Vol. 30, No. 10, pp. 1379–1389, 1999

Printed in Great Britain
0021-8502/99/$ - see front matter

A RECIPE FOR IMAGE CHARACTERIZATION OF FRACTAL-LIKE AGGREGATES

A. M. Brasil, T. L. Farias* and M. G. Carvalho

Department of Mechanical Engineering, Instituto Superior Técnico, Universidade Técnica de Lisboa, Av. Rovisco Pais 1049-001 Lisboa, Portugal

(*First received* 10 *October* 1998; *and in final form* 16 *February* 1999)

Abstract—In the present paper a simple and straightforward recipe for characterizing the structural and fractal properties of aggregates from their projected images is presented. Starting from geometrical properties that are directly measured from the projected image—such as primary particle mean diameter, maximum projected length, projected area, and overlap coefficient—important three-dimensional properties including number of primary particles in an aggregate, radius of gyration, aggregate surface, or fractal dimensions, D_f and k_g, can be inferred. Expressions proposed in the recipe to relate three dimensional with projected properties were obtained from an extensive investigation of the structure of numerically simulated cluster–cluster fractal-like aggregates. This involved the simulation of statistically significant populations of aggregates having appropriate fractal properties and prescribed numbers of primary particles per aggregate in order to characterize three-dimensional morphological properties of aggregates. Specific ranges of aggregate properties considered were as follows: number of primary particles per aggregate up to 512, fractal dimension, $D_f \approx 1.78$, overlap coefficient in the range 0–0.33 and fractal pre factor between 1.5 and 3.1. © 1999 Elsevier Science Ltd. All rights reserved

NOMENCLATURE

A_a	projected area of an aggregate
A_p	cross-sectional area of a primary particle, $A_p = (\pi d_p^2/4)$
a	primary particle radius
C_{ov}	overlap coefficient
d_p	diameter of primary particle
D_f	aggregate fractal dimension
k_a	projected area pre factor
k_g	fractal pre-factor (based on R_g, see equation (1))
k_L	fractal pre-factor based on L
L	projected maximum length of aggregate
N	number of primary particles in an aggregate
R_g	radius of gyration of an aggregate
S_a	aggregate total exposed surface

Greek symbol

α_a	projected area exponent

1. INTRODUCTION

Aggregated particles, such as aerosols, are present in a wide range of engineering fields such as combustion processes for power generation and pigment production. These agglomerates are usually composed of fine primary particles (monomers) that coagulate to form irregular clusters. Because of complex nucleation and aggregation processes most combustion generated agglomerates have a broad size distribution (see Köylü and Faeth, 1992; Megaridis and Dobbins, 1990 and references cited therein). Although different in their size, shape, radius of gyration and particle density, these aggregates exhibit complex geometry that fortunately can be characterized as mass fractals; that is, the number of primary particles per aggregate, N, scales with the radius of gyration, R_g, as follows:

$$N = k_g(R_g/a)^{D_f} \tag{1}$$

*Author to whom correspondence should be addressed.

where k_g is the fractal pre-factor (also known as the structural coefficient) and D_f the fractal dimension. The term "fractal dimension" may be questioned when the aggregate size is small since deviations from the asymptotic value can become significant. However, the term has been adopted in the present work following the suggestion of several authors (Megaridis and Dobbins, 1990; Cai *et al*., 1995; Köylü *et al*., 1995a, b). Although most studies in the past have considered the fractal dimension as the key property to characterize fractal-like aggregates, Wu and Friedlander (1993), Cai *et al*. (1995) and, more recently, Köylü *et al*. (1995a) and Oh and Sorensen (1997) have shown that both the fractal dimension and the pre-factor must be correctly known in order to fully define the fractal structure of a specific aggregate. This seems reasonable from equation (1) which indicates that the fractal dimension alone is not sufficient to determine the radius of gyration of an aggregate assuming that the radius of the monomers and the number of monomers within the aggregate are known. Unfortunately, the knowledge of these two variables is rarely known, thus most investigators have been forced to study projected images of collections of aggregates in order to better understand their morphology and estimate both N and R_g. In fact, most of past studies of aggregate morphology have been based on *ex situ* transmission electron microscope (TEM) or/and *in situ* light scattering measurements, in particular for flame generated particles. For example studies of Medalia and Heckman (1969, 1971) have investigated the morphology of collected black carbon particles. Samson *et al*. (1987) and Megaridis and Dobbins (1990) were pioneers in investigating the structure of soot aggregates, followed by the studies of Köylü *et al*. (1992, 1994, 1995a, b), Sorensen *et al*. (1992a, b) and Cai *et al*. (1995), among others. The majority of these studies involved analysis of TEM projected images of aggregates, thus requiring simple relationships between the two-dimensional visible information and the real three-dimensional properties of the aggregates. Nelson *et al*. (1990) and more recently Köylü *et al*. (1995b) have reported important information in that field but limited their studies to the particular case of soot aggregates without taking into consideration important properties such as aggregate total surface and overlapping of primary particles. Oh and Sorensen (1997) investigated the latter subject, in particular the effect of partial overlapping on the expressions used to infer three-dimensional properties from projected images. However, no attempt was made to generalize these findings for a wider range of structural properties and overlap coefficients.

In summary, most structural and geometrical properties of aggregates are commonly unknown and therefore obtained from projected images. Based on these facts, the present investigation seeks to contribute to a better understanding of the structure of fractal like aggregates. In order to achieve those objectives a recipe is presented to characterize the structural and fractal properties of aggregates from their projected images. Starting from geometrical properties that are measured either directly from the image or through the use of standard image characterization software important three-dimensional properties can be obtained, namely the number of primary particles in an aggregate, N, radius of gyration, R_g, aggregate surface, S_a, or fractal dimensions, D_f and k_g. Expressions proposed in the recipe to relate three dimensional with projected properties were obtained from an extensive investigation of the structure of numerically simulated cluster–cluster fractal-like aggregates. This involved the simulation of statistically significant populations of aggregates having appropriate fractal properties and prescribed numbers of primary particles per aggregate in order to characterize three-dimensional morphological properties of aggregates. Specific ranges of aggregate properties considered were as follows: number of primary particles per aggregate, N, up to 512, fractal dimension, D_f, of 1.78, overlap coefficient in the range 0–0.33 and fractal pre-factor between 1.5 and 3.1.

The paper begins with a description of the numerical simulation procedure adopted to generate the fractal-like aggregates. The population of aggregates used for the present investigation is then fully characterized in particular their fractal and structural properties. The paper follows by an investigation of relationships between the properties of actual and projected fractal-like aggregates emphasizing the effects of primary particle partial overlapping and aggregate size. Specific properties addressed included actual three-dimensional radius of gyration, number of monomers per aggregate and fractal dimensions. Further on

a simple but powerful recipe for obtaining three-dimensional properties of aggregates from projected images is presented.

2. NUMERICAL SIMULATION OF FRACTAL-LIKE AGGREGATES

Various procedures to construct agglomerates composed of spherical primary units have been discussed by Jullien and Botet (1987) and Botet and Jullien (1988). These methods are based on simple algorithms that mimic cluster–cluster or particle–cluster aggregation processes due to Brownian motion. Due to their relative simplicity, several investigators (e.g. Vold, 1963; Hutschinson and Sutherland, 1965; Witten and Sander, 1981, 1982; Meakin, 1983a, b) have adopted particle–cluster methods. A more physically based method was developed by Mountain and Mulholland (1988) who generated soot aggregates using a numerical simulation involving cluster–cluster aggregation based on the solution of the Langevin equations. This approach yields fractal-like aggregates that satisfy the power-law relationship of equation (1) with D_f ca. 1.9 and k_g roughly 1.5 for $N > 10$. However, a larger sample of aggregates was needed for the present study, and it was also required that the present aggregates have specific fractal dimensions and overlap coefficient. As a result, an alternative simulation method previously used by Farias *et al.* (1995, 1996a, b, 1997) and Köylü *et al.* (1995b) was applied during the present investigation.

The aggregate simulation method involved creating a population of aggregates by cluster–cluster aggregation using a sequential algorithm that satisfies equation (1) intrinsically, rather than performing numerical simulations based on Langevin dynamics along the lines of the approach used by Mountain and Mulholland (1988). For pre-specified values of D_f and k_g, the aggregate generation process was initiated by randomly attaching individual and pairs of particles to each other, assuming uniform distributions of the point and orientation of attachment, while rejecting configurations where primary particles intersected. The radius of gyration of the new aggregate was calculated based on the known positions of the primary particles, and checked to see if equation (1) was satisfied for the fractal dimension and pre-factor selected. This procedure was continued in order to form progressively larger aggregates that obeyed the statistical relationships of mass fractal objects. As a default a hierarchical approach was used where only clusters having the same number of primary particles (or a similar number if N was odd) were joined together (Jullien and Botet, 1987). Nevertheless, if desired, the model was capable of creating non-hierarchical aggregates.

3. RESULTS AND DISCUSSION

3.1. *Preliminary considerations*

In the present study a well-defined population of fractal-like aggregates was desired. Therefore, the simulated aggregates were generated using pre-defined values for both the fractal dimension, D_f, and pre-factor, k_g. Although the fractal dimension has received considerable attention in the past, the selection of universal values for the structural coefficient for cluster–cluster (as well as particle–cluster) aggregates is still a controversial issue. Wu and Friedlander (1993) and, more recently, Köylü *et al.* (1995a) have unified most of experimental and numerical data reported on this property. For example, for cluster-cluster aggregates results published in the literature for k_g indicate values between 1.23 (Cai *et al.*, 1995) and 3.47 (Samson *et al.*, 1987). The range of results published varies by more than 200% that clearly shows that this issue deserves more attention. In spite of the range of values published, it was noted that results based on numerically simulated aggregates are systematically inferior to k_g values inferred from experimental data. Oh and Sorensen (1997) have investigated the effect of overlap between primary particles on the fractal properties concluding that the fractal dimension and particularly the fractal pre-factor may vary considerably with the rate of overlapping. However, no final conclusion regarding the discrepancies between experimental results and numerical finding were achieved. Our

present results will show that the large discrepancies between the values reported for k_g appear to be related with the partial overlapping of primary particles that leads to an increase of k_g while keeping the fractal dimension approximately constant. Therefore, it can be concluded that aggregates without overlapping should be simulated having lower values of k_g while as overlapping increases, k_g will also increase as systematically observed by several authors.

In summary, and in order to establish reference values for the population of simulated aggregates required for the present study, cluster–cluster aggregates were built using $k_g = 1.5$ which lead to $D_f \approx 1.78$.

Partial overlapping of primary particles that unavoidably exists between two (or more) touching particles in real combustion generated aggregates was also considered in the present work. An overlap parameter, C_{ov}, was defined as follows:

$$C_{ov} = (d_p - d_{ij})/(d_p), \tag{2}$$

where d_{ij} represents the distance between two touching particles while d_p is the diameter of primary particles (see Fig. 1). If $C_{ov} = 0$ the primary particles are in point contact while $C_{ov} = 1$ total sintering took place indicating that every couple of neighbors merged into one. Numerically, overlapping was accounted for by progressively increasing the diameters of the primary particles within an aggregate while maintaining the position of the center of the particle, followed by a scaling correction to keep the same reference value for particle diameter. Projected images of a typical aggregate having $N = 128$, and $C_{ov} = 0$, 0.15, 0.25 and 0.33 constructed using the present simulation procedure are illustrated in Fig. 1.

The population of simulated aggregates involved N in the range 8–512, considering 7 different aggregate sizes (Fig. 2 shows a log–log plot of R_g/a versus N for the population of aggregates generated yielding the fractal dimensions). Results obtained for each aggregate size class were averaged over 32 different aggregates to yield a total sample of 224 aggregates. In addition each aggregate was observed in four randomly chosen orientations. This sample size was established in order to obtain a numerical uncertainty (95% confidence) less than 10% for the different variables investigated throughout the present study. In order to fix ideas, a mean primary particle diameter of unity was used for the simulations. However, present results are normalized by a, d_p or A_p, and such normalized results become therefore independent of d_p. Finally, with the purpose of simplifying the amount of data plotted in the figures, only mean values are shown for each aggregate size class.

3.2. *Projected properties required*

To follow the methodology (recipe) presented later on in Section 3.4, several projected properties are required, namely the mean primary particle diameter, d_p, the aggregate

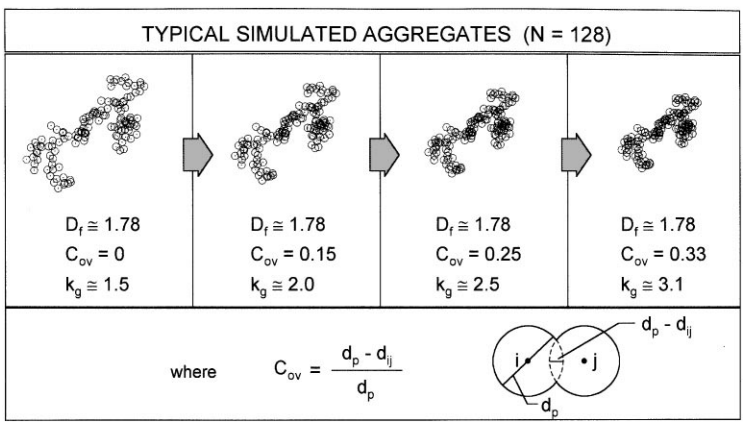

Fig. 1. Projected images of a typical numerically simulated aggregate having $N = 128$, and $C_{ov} = 0$, 0.15, 0.25 and 0.33.

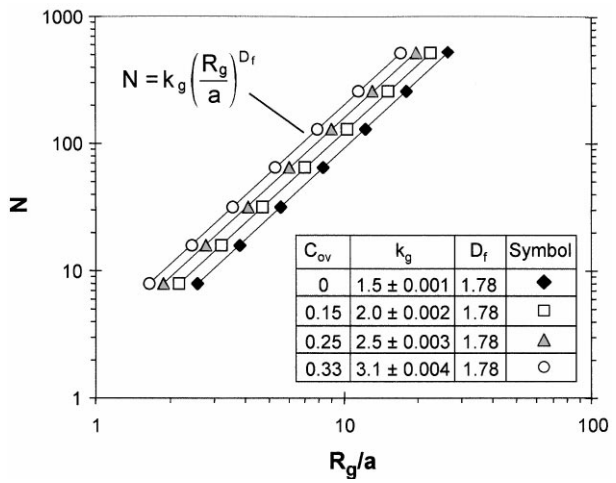

Fig. 2. Number of particles in aggregates as a function of radius of gyration normalized by particle radius, yielding the fractal dimension and fractal pre-factor of simulated aggregates with different overlap parameter, C_{ov}.

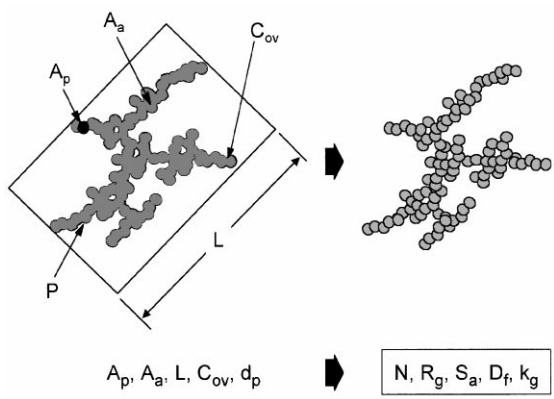

Fig. 3. Main variables required measuring from the projected image to infer three-dimensional structural properties.

projected area, A_a, (or perimeter, P) aggregate projected maximum length, L, and mean overlap coefficient, C_{ov} (see Fig. 3). While the maximum projected length is a simple and straightforward property to measure the remaining ones may require some additional help. Mean primary particle diameter requires the selection of several particles from the projected image as in most cases this property follows a Gaussian distribution with standard deviations up to 25% (Köylü and Faeth, 1992). Current available software for image analysis give either the projected area, A_a, of the image or (and) the perimeter, P. Projected area has been adopted in the past by most researchers to infer three-dimensional properties. Therefore, our results will be developed based on the projected area. Finally, the overlap parameter should be obtained from the projected image. Unfortunately, this is not directly obtained because the projection of the image of a three-dimensional aggregate leads to additional overlapping. To overcome this problem we have observed more than 300 couples and compared the projected overlap coefficient with the real values that were assigned while constructing the aggregates. Results obtained indicated that the real overlap parameter scales with the projected one in the following manner:

$$C_{ov} = \zeta_1 C_{ov,proj}\text{-}\zeta_2, \quad \text{where } \zeta_1 = 1.1 \pm 0.1 \text{ and } \zeta_2 = 0.2 \pm 0.02. \tag{3}$$

3.3. *Relationships between three-dimensional and projected properties*

As previously mentioned, although the knowledge of the three-dimensional properties of the structure of aggregates is required in many applications, it is not practical to estimate these properties experimentally. One powerful way of avoiding the cumbersome task of analyzing the three-dimensional properties of aggregates is to establish relationships between the actual and projected properties that can be easily measured. The present section is dedicated to establishing several relationships that will help identifying the size of the aggregate (number of primary particles, N), the fractal dimension and pre-factor, the radius of gyration and the surface area from the required simple measurable properties previously described. These expressions will be the main ingredients of the recipe presented in Section 3.4.

3.3.1. *Number of primary particles.* The first property studied in this section is the number of primary particles in an aggregate, N. A potentially useful way to obtain N is through the projected area of the aggregate. In fact, several workers have suggested the following relationship between the projected area of an aggregate, A_a, and N (see Köylü *et al.*, 1995a and references cited therein):

$$N = k_a(A_a/A_p)^{\alpha_a}, \tag{4}$$

where α_a is an empirical projected area exponent and k_a is a constant. Our numerical results are plotted in Fig. 4. As can be seen, this power correlation fits very well the numerical simulations for the complete range of N and C_{ov} covered. In addition, results obtained for aggregates having non-overlapping neighboring particles (namely $\alpha_a = 1.08 \pm 0.003$ and $k_a = 1.10 \pm 0.005$) are in very close agreement with previous values reported by several authors.

In fact, a value of $\alpha_a = 1.08$ is consistent with the results of a computer simulation of ballistic cluster–cluster aggregation by Meakin *et al.* (1989) in which $7 < N < 2500$. Using stereopairs observation, Samson *et al.* (1987) directly ascertained N for a collection of 39 aggregates for $5 < N < 162$ that were captured from the plume of a smoking acetylene flame. The values of A_a for the same population of Samson *et al.* (1987) were determined by Megaridis and Dobbins (1990) and resulted in the determination $\alpha_a = 1.09$. More recently, results proposed by Köylü *et al.* (1995b) for soot fractal aggregates based on both numerical and experimental data have confirmed that the power-law correlation of equation (4)

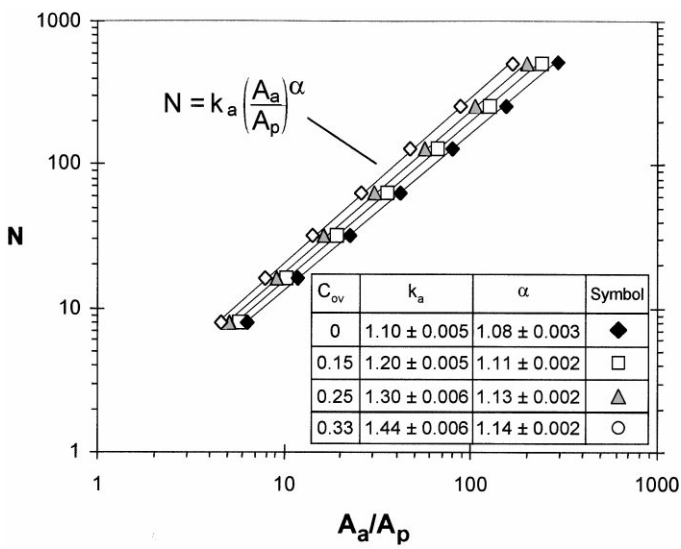

Fig. 4. Number of primary particles as a function of projected area ratio for simulated aggregates having different overlap parameters.

provides an excellent fit of the data. Their least-squares fit values were $\alpha_a = 1.10$ and $k_a = 1.16$ with standard deviations of 0.002 and 0.01, respectively. For overlap coefficients greater than zero the power-law correlation continues to exhibit an excellent fit with both coefficients showing a tendency to increase with C_{ov}.

3.3.2. *Radius of gyration.* As noted earlier, for example through equation (1), the radius of gyration is an important aggregate property. Several authors have suggested that L, the maximum projected length of an aggregate, could act as a substitute of R_g in the fundamental fractal relationship of equation (1). For example, Puri *et al.* (1993) using the measurements of Samson *et al.* (1987) reported $L/(2R_g) = 1.78$ although a very limited sample was used. Köylü *et al.* (1995b) have investigated both experimentally and numerically the structural and fractal properties of soot aggregates and suggested $L/(2R_g) = 1.49$ for aggregates with $N > 100$. More recently, Oh and Sorensen (1997) presented for their numerically simulated aggregates $L/(2R_g) = 1.45$. Present results are illustrated in Fig. 5 where plots of $L/(2R_g)$ as a function of N are shown for aggregates with different overlap coefficients. For the range of N and C_{ov} covered, the variation of $L/(2R_g)$ is small and, for practical use, the following value (independent of both parameters) is suggested:

$$L/(2R_g) = 1.50 \pm 0.05. \tag{5}$$

These conclusions are very useful because they indicate that the actual radius of gyration of an aggregate can be extracted from L, a simple and measurable quantity. In addition they support the approach suggested by Köylü *et al.* (1995a) to extract the fractal dimensions from L and particle radius, a, as discussed later on when investigating the fractal properties.

3.3.3. *Surface area.* Another relevant property of open structure materials such as fractal-like aggregates is the real surface area that is progressively reduced as the overlap parameter increases. This property is directly related to deposition mechanisms, oxidation rates or chemical reactions that may occur at the aggregate surface. Figure 6 includes results obtained (symbols) concerning the effect of overlapping on the reduction of the total surface area for different aggregate sizes. Results indicate that the effect of aggregate size vanishes as N increases. Based on these trends for aggregates having $N \geqslant 10$, we suggest the following expression (lines on Fig. 6) to estimate aggregate surface area:

$$S_a/S_{a(C_{ov}=0)} = 1 - \phi C_{ov}\,(1 - 1/N) \quad \text{where } \phi = 1.3. \tag{6}$$

It is interesting to note that if the coordination number (number of contacts per primary particles) were 2 for all particles (such as an infinite long chain) ϕ would be equal to 2. Finally, for large N equation (6) can be simplified to $S_a/S_{a(C_{ov}=0)} = 1 - 1.3C_{ov}$.

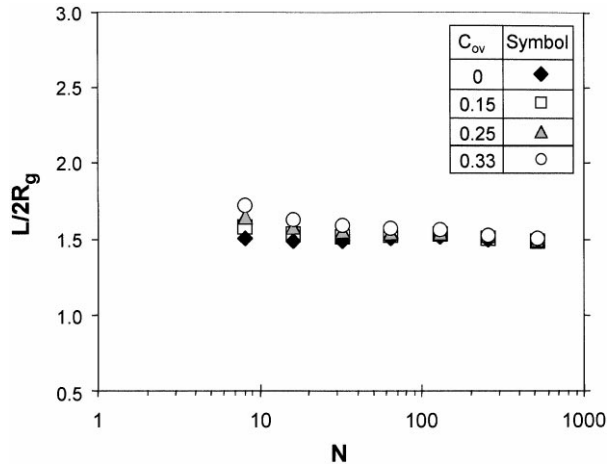

Fig. 5. Radius of gyration as a function of aggregate size for simulated aggregates having different overlap parameters.

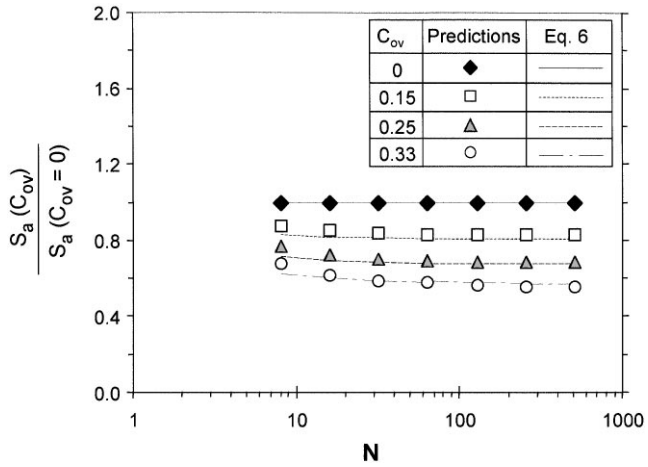

Fig. 6. Aggregate surface area as a function of aggregate size for simulated aggregates having different overlap parameters.

3.3.4. *Fractal properties.* As discussed earlier, the simulated aggregates were mass fractal-like, satisfying equation (1) as shown in Fig. 2. Unfortunately, a direct evaluation of the fractal properties from equation (1) requires extensive data reduction of stereopairs. Information of this type is not often available so that several simplified methods based on projected aggregate dimensions have been developed, as discussed by Jullien and Botet (1987). Nelson *et al.* (1990) presented a method to obtain the fractal dimension from projected images of smoke aggregates. Although this method is theoretically based it is not simple to use as it requires the projected fractal dimension. More recently, Köylü *et al.* (1995a) suggested the following expression to obtain D_f from the slope of a log–log plot of N versus $L/2a$ (where L is the maximum projected length of the aggregate):

$$D_f = D_{fL} = \ln (N/k_L)/\ln (L/2a). \tag{7}$$

While D_{fL} represents the slope, k_L (a correlation pre-factor similar to k_g) determines the magnitude of the least-square linear fit to the data in the N versus $L/2a$ plot. Further on, the authors suggest that the structural coefficient, k_g, is then obtained using the following expression:

$$k_g = k_L \left(\frac{D_f + 2}{D_f} \right)^{D_f/2}. \tag{8}$$

If equation (7) is adopted, i.e. the fractal dimension of the aggregate is directly obtained from the slope of a log–log plot of N versus $L/2a$, then, using equations (1), the following alternative expression for k_g is obtained:

$$k_g = k_L (L/2\ R_g)^{D_f}, \tag{9}$$

where according to equation (5), $L/(2R_g) \approx 1.5$. Therefore, k_g can be obtained directly from the log–log plot of N versus $L/2a$ as follows:

$$k_g = k_L\ (1.5)^{D_f}. \tag{10}$$

Although it is out of the scope of the present study to investigate the actual values of both k_g and D_f obtained from the simulated aggregates as they were initially imposed, our simulated aggregates can, however, be used to confirm the applicability of these useful expressions.

Figure 7 shows a log–log plot of N versus $L/2a$ for the population of aggregates generated yielding the fractal dimensions k_L and D_{fL}. A summary of the results obtained for these two parameters as a function of C_{ov} is shown in Table 1. Also included in this table are the results

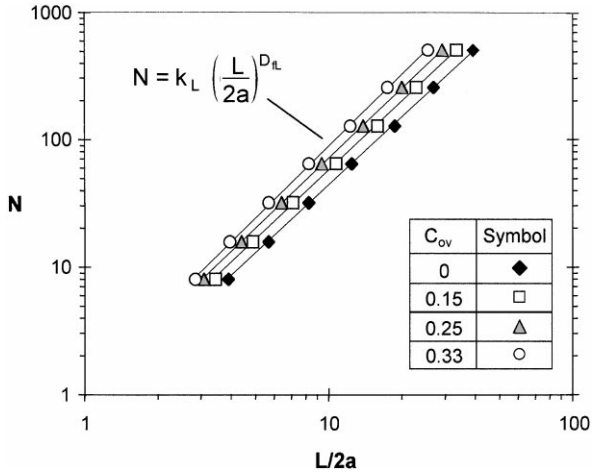

Fig. 7. Number of primary particles as a function of maximum projected length for simulated aggregates yielding the fractal dimensions.

Table 1. Fractal dimensions obtained from the slope of a log–log plot of N versus $L/2a$ (Fig. 7) together with equations (7) and (8) or (10)

C_{ov}	D_{fL}	D_f (Fig. 2)	k_L	k_g equation (8)	k_g equation (10)	k_g (Fig. 2)
0	1.78 ± 0.0001	1.78	0.73 ± 0.005	1.41	1.48	1.49
0.15	1.81 ± 0.0001	1.78	0.87 ± 0.006	1.71	1.81	2.00
0.25	1.84 ± 0.0001	1.78	1.00 ± 0.007	1.97	2.11	2.52
0.33	1.87 ± 0.0001	1.78	1.15 ± 0.008	2.27	2.45	3.12

obtained for k_g and D_f using equations (7), (8) and (10) as well as the real values exhibited by the population of aggregates used (see Fig. 2). Results indicate that the expressions proposed by Köylü *et al.* (1995a) as well as equation (10) seems to give very good estimates of the actual fractal properties of fractal-like cluster–cluster aggregates, i.e. within 10–15% when overlapping is not a dominant mechanism. However, as C_{ov} increases deviations between real values and estimated results of k_g from both approaches start to become significant. For the upper limit of $C_{ov} = 0.33$, deviations between real and estimated values of the fractal pre-factor reach 25 and 20% when equations (8) and (10) are used, respectively.

In conclusion fractal properties can be obtained from projected data as long as overlapping mechanisms are relatively low which is the case of most combustion-generated particles (such as soot).

3.4. *Recipe for image characterization of fractal-like aggregates*

Having established the required relationships between projected measurable properties and three-dimensional data we now present the main steps of the recipe:

(i) Measure from the projected images the overlap parameter, C_{ov}. Identify several (ca. 48) couples (if possible near the tips of the projected image) and measure $C_{ov,proj}$. Use equation (3) to obtain C_{ov}.

(ii) From the projected image measure L, a and A_a. While maximum lengths and projected areas are given by standard image characterization software, the primary particle radius has to be measured after identifying several individual monomers and calculating the mean value.

(iii) Estimate N using equation (4) (A_a, a and C_{ov} as input);

(iv) Estimate R_g using equation (5) (a and L as input);

Table 2. Effect of resting position (i.e. number of contact points with surface) on the coefficients of the expressions proposed to extract aggregate number of primary particles, and fractal dimensions

Number of contact points	$N = k_a (A_a/A_p)^{\alpha_a}$		$N = k_L (L/2a)^{D_{fL}}$	
	k_a	α_a	k_L	D_{fL}
1 (Suspended)	1.10	1.09	0.73	1.78
2	1.02	1.10	0.63	1.80
3	0.97	1.11	0.63	1.80

(v) Estimate S_a using equation (6) (A_a, a, N and C_{ov} as input);

(vi) For the family of aggregates in study plot on a log–log scale N versus $L/2a$. Estimate best fit and obtain D_{fL} (the slope) and k_L (the magnitude of the least-square linear fit to the data). Obtain the fractal dimensions D_f, and k_g using equations (7) and (10).

3.5. *Anysotropic effects on projected image analysis*

In the present work aggregates were considered to be suspended. However, in many practical situations, the collection of the aggregates may force them to reach a resting position with more that one contact point with the surface. This is the case if the bond between the touching primary particle and the surface is not rigid or if additional forces act on the aggregate leading to a rolling effect. This effect will contribute to systematic deviations of some of the projected properties considered. For example, the maximum projected length of a suspended aggregate (i.e. having one contact point) is expected to be, in average, less than the value obtained from the same aggregate after reaching a more stable position (i.e. with more than one contact point). Oh and Sorensen (1997) describe this effect while analyzing the radius of gyration of an ellipsoid. In the present section this effect is addressed and results are presented for the situation where the aggregate after reaching the collecting surface rolls until 2 and finally 3 contact points are reached. This was numerically done by simulation the continuous movement of the aggregate assuming that an external force (for example due to gravity, thermophoresis or an electromagnetic field) perpendicular to the collecting surface is acting on the aggregate. In Table 2 results for the different expressions presented in our recipe are compared for the one (i.e. suspended aggregates), two and three contact points.

As can be concluded rolling of the aggregates until a more stable position is reached contributes to larger projected areas and maximum projected length L. Thus, if these effects are not properly accounted for, the number of primary particles, N, and the fractal pre-factor k_g may be slightly overestimated (ca. 10–15%).

4. CONCLUSION

In the present paper a simple and straightforward recipe for characterizing the structural and fractal properties of aggregates from their projected images is presented. Starting from geometrical properties that are directly measured from projected images important three-dimensional properties can be inferred. The expressions proposed in the recipe to relate three dimensional with projected properties were obtained from an extensive investigation of the structure of numerically simulated cluster–cluster fractal-like aggregates. The main conclusions of the present work can be summarized as follows:

(1) Although exhibiting a complex structure, the morphology of combustion generated aggregates can be characterized in a fairly simple and straightforward manner due to their fractal-like nature.

(2) The radius of gyration of an aggregate can be inferred simply by measuring the maximum projected length of the aggregate.

(3) Number of primary particles in an aggregate can be obtained by knowing the projected area and mean primary particle diameter.

(4) For large N, the reduction of the aggregate surface area due to partial overlapping between primary particles is solely a function of the overlap coefficient C_{ov}.

(5) Fractal properties can be obtained directly from the projected data as long as the overlapping mechanisms are not dominant.

Acknowledgements—A. M. Brasil would like to acknowledge the scholarship of Conselho Nacional de Desenvolvimento Científico e Tecnológico—CNPq. The authors would also like to acknowledge the valuable comments and suggestion offered by Prof. D. E. Rosner and Dr. Y. Xing from Yale University and Dr. Ümit Köylü from Florida International University.

REFERENCES

Botet, R. and Jullien, R. (1988) A Theory of Aggregating Systems of Particles: the Clustering of Clusters Process. *Ann. Phys. Fr.* **13,** 153–231.

Cai, J., Lu, N. and Sorensen, C. M. (1995) Analysis of fractal cluster morphology parameters: structural coefficient and density autocorrelation function cutoff. *J. Colloid Int. Sci.* **171,** 470–473.

Farias, T. L., Carvalho, M. G., Köylü, Ü. Ö. and Faeth, G. M. (1995) Computational evaluation of approximate Rayleigh–Debye–Gans/fractal-aggregate theory for the absorption and scattering properties of soot. *J. Heat Transfer* **117,** 152–159.

Farias, T. L., Köylü, Ü. Ö. and Carvalho, M. G. (1996a) Effects of polydispersity of aggregates and primary particles on radiative properties of simulated soot. *J. Quantitative Spectroscopy and Radiative Transfer* **55** (3), pp. 357–371.

Farias T. L., Carvalho, M. G. and Köylü, Ü. Ö. (1996b) The range of validity of the Rayleigh–Debye–Gans/fractal-aggregate theory for computing optical properties of fractal-like aggregates. *Appl. Opt.* **35** (33), 6560–6567.

Farias, T. L., Carvalho, M. G. and Köylü, Ü. Ö. (1997) Radiative heat transfer in soot-containing combustion system with aggregates. *Int. J. Heat and Mass Transfer* **41** (17), 2581–2587.

Hutchison, H. P. and Sutherland, D. N. (1965) An open-strutured random solid. *Nature* **206,** 1036–1037.

Jullien, R. and Botet, R. (1987) *Aggregation and Fractal Aggregates.* World Scientific Publishing Co., Singapore, pp. 46–60.

Köylü, Ü. Ö. and Faeth, G. M. (1992) Structure of overfire soot in buoyant turbulent diffusion flames at long residence times. *Combust. Flame* **89,** 140–156.

Köylü, Ü. Ö. and Faeth, G. M. (1994) Optical properties of soot in buoyant laminar diffusion flames at long residence times. *J. Heat Transfer* **116,** 152–159.

Köylü, Ü. Ö., Xing, Y. and Rosner, D. E. (1995a) Fractal morphlogy analysis of combustio-generated aggregates using angular light scattering and electron microscope images. *Langmuir* **11** (12), 4848–4854.

Köylü, Ü. Ö., Faeth, G. M., Farias, T. L. and Carvalho, M. G. (1995b) Fractal and projected structure properties of soot aggregates. *Combust. Flame* **100,** 621–633.

Meakin, P. (1983a) Diffusion controlled cluster formation in two, three, and four dimensions. *Phys. Rev. A* **27,** 604–607

Meakin, P. (1983b) Diffusion-controled cluster formation in 2–6-dimensional space. *Phys. Rev. A* **27,** 1495–1507.

Meakin, P., Donn, B. and Mulholand, G. W. (1989) Collisions between point masses and fractal aggregates. *Langmuir* **5,** 510.

Medalia, A. I. and Heckman, F. A. (1969) Morphology of aggregates—II. Size and shape factors of carbon black aggregates from electron microscopy. *Carbon* **7,** 567.

Medalia, A. I. and Heckman, F. A. (1971) Morphology of aggregates—VII. Comparison chart for electron microscopic determination of carbon black aggregates morphology. *J. Colloid Int. Sci.* **36** (2), 173–190.

Megaridis, C. M. and Dobbins, R. A. (1990) Morphological description of flame-generated materials. *Combust. Sci. Technol.* **71,** 95–109.

Mountain, R. D. and Mulholland, G. W. (1988) Light scattering from simulated smoke agglomerates. *Langmuir* **4,** 1321–1326.

Nelson, J. A., Crookes, R. J. and Simons, S. (1990) On obtaining the fractal dimension of a 3D cluster from its projection on a plane—application to smoke agglomerates. *J. Phys D: Appl. Phys.* **23,** 465–468.

Oh, C. and Sorensen, C. M. (1997) The effect of overlap between monomers on the determination of fractal cluster morphology. *J. Colloid Int. Sci.* **193,** 17–25.

Puri, R., Richardson, T. F., Santoro, R. J. and Dobbins, R. A. (1993) Aerosol dynamic processes of soot aggregates in a laminar ethene diffusion flame. *Combust. Flame* **92,** 320–333.

Samson, R. J., Mulholand, G. W. and Gentry, J. W. (1987) Structural analysis of soot agglomerates. *Langmuir* **3** (2), 272–281.

Sorensen, C. M., Cai, J. and Lu, N. (1992a) Test of static structure factors for describing light scattering from fractal soot aggregates. *Langmuir* **8,** 2028–2069.

Sorensen, C. M., Cai, J. and Lu, N. (1992b) Light-scattering measurements of monomer size, monomers per aggregate, and fractal dimension for soot aggregates in flames. *Appl. Opt.* **31,** 6547–6557.

Vold, M. J. (1963) Computer simulation of floc formation in a colloidal suspension. *J. Colloid Sci.* **18,** 684–695.

Witten, T. A. and Sander, L. M. (1981) Diffusin-limited aggregation, a kinetic critical phenomenon. *Phys. Rev. Lett.* **47,** 1400–1403.

Witten, T. A. and Sander, L. M. (1982) Diffusin-limited aggregation. *Phys. Rev.* B **27,** 5685–5697.

Wu, M. and Friedlander, S. K. (1993) Note on the power-law equation for fractal-like aerosol agglomerates. *J. Colloid Int. Sci.* Vol. **159,** 246–248.